Chinese Chemical Letters 33 (2022) 2021–2025

Contents lists available at ScienceDirect

Chinese Chemical Letters

journal homepage: www.elsevier.com/locate/cclet

Noble metal aerogels rapidly synthesized by ultrasound for electrocatalytic reaction

Yueyue Yuan[a], Huan Zhao[a], Wenxia Xv[a], Dan Zhang[b], Zuochao Wang[a], Hongdong Li[a], Yingnan Qin[a], Shaoxiang Li[b], Jianping Lai[a,*], Lei Wang[a,b,*]

[a] Key Laboratory of Eco-chemical Engineering, Key Laboratory of Optic-electric Sensing and Analytical Chemistry of Life Science, Taishan Scholar Advantage and Characteristic Discipline Team of Eco Chemical Process and Technology, College of Chemistry and Molecular Engineering, Qingdao University of Science and Technology, Qingdao 266042, China
[b] Shandong Engineering Research Center for Marine Environment Corrosion and Safety Protection, College of Environment and Safety Engineering, Qingdao University of Science and Technology, Qingdao 266042, China

ARTICLE INFO

Article history:
Received 17 June 2021
Revised 29 September 2021
Accepted 30 September 2021
Available online 4 October 2021

Keywords:
Ultrasonic
Aerogels
Noble metals
Rapid synthesis
Electrocatalysis

ABSTRACT

Noble metal aerogels (NMAs), belonging to the porous material, have exhibited excellent catalytic performance. Although the synthesis method continues to improve, it still exists some problems which hindered the experimental process, such as high concentration of noble metal precursors, long synthesis cycle, expensive production cost, and uncontrollable ligament length. In this work, ultrasonic wave and reducing agent $NaBH_4$ were simultaneously applied to gelation process. With the cavitation of ultrasound, it can generate huge energy with heating and stirring, thus gelation reaction proceeded quickly, and even completed the process in only a few seconds, that is much faster than the recorded. A wide concentration range was successfully expanded from 0.02 mmol/L to 62.5 mmol/L. Further, we extended this method to a variety of noble metal elements (Au, Ru, Rh, Ag, Pt, Pd), and this method is adaptive for the synthesis of single metal aerogels (Au, Ag, Ru, Rh, Pd), bimetal and trimetal aerogels (Au-Ag, Au-Rh, Au-Ru, Au-Pt, Au-Pd, Au-Pt-Pd). In addition, the ligament size of alloy aerogels are 10 nm or less. Moreover, their brilliant properties were demonstrated in hydrogen evolution reaction (HER) and ethanol oxidation reaction (EOR).

With the progress and development of society, the depletion of fossil fuels, environmental problems have become increasingly serious, and energy conversion problems need to be solved urgently [1]. Under this background, electrocatalysis has been gradually developed [2], and porous materials [3] have attracted extensive attention of researchers due to their special structure and outstanding catalytic activity. As a new type of porous material [4], aerogels have low density and large specific surface area [5–13]. Among them, the noble metal aerogels (NMAs), despite expensiveness with respect to other materials, still play an indispensable role in a wide range of fields. For example, they have excellent performance in the catalytic reaction of energy and environment [14–18]. NMAs have some of the characteristics of foams [19], such as three-dimensional (3D) networks and self-supporting overall structure, large specific surface area, high porosity and more active sites exposed [20–23]. Besides, they possess unique physical and chemical properties of noble metals, which are conducive to the rapid transfer of electrons in the channel, and have excellent catalytic performance [14,20,24-28]. Consequently, they attract more and more attention of researchers, and are applied to many aspects, especially the bright application prospect in electrocatalysis.

In recent years, with the in-depth research on NMAs, great progress has been made in the synthesis and preparation of NMAs. Traditionally, nanoparticles are gelled by the addition of destabilizing agents, and then aerogels are obtained through centrifugation and supercritical technology [20,29,30]. The two steps of nanoparticle synthesis and destabilization separate operations are conducive to control of nanostructures well [11,31,32]. Afterward, Liu *et al.* studied a one-step method to synthesize NMAs, using $NaBH_4$ to directly gel the metal salt solution, which greatly improved the purity of the aerogels [33–35]. Meanwhile, the gelation time was shortened from 1 to 4 weeks to days or even minutes [33]. At present, there are more mature methods to destabilize colloidal metal solutions, such as salting out and stirring [36], adding non-stabilizer [37], heating [33]. The ionic effects [30], lig-

* Corresponding authors.
E-mail addresses: jplai@qust.edu.cn (J. Lai), inorchemwl@126.com (L. Wang).

https://doi.org/10.1016/j.cclet.2021.09.104
1001-8417/

and effects [35], the synthesis of NMAs induced by excess reducing agent [35], and the NMAs synthesized by freeze-thaw methods are further clarified [38,39]. Despite the synthesis methods have been continuously improved, there are still some problems which hinder the experimental process, such as long synthesis cycle, high concentration of noble metal precursors, expensive production cost and uncontrollable ligament length. Hence, it is necessary to explore an approach that can be highly effective, rapid, environmentally friendly to synthesize aerogels. Ultrasonic machines are cheap and common.

The ultrasonic waves have strong penetrability in water, and can produce cavitation, which generates local high temperature and pressure with heating and stirring for the reaction system, thus speeding up the reaction. Besides, $NaBH_4$ is ionized into Na^+ and BH_4^- in water. Na^+ adjusts the fusion mode of particles, while BH_4^- in the system can not only reduce metal ions, but also increase instability and collision between metal nanoparticles through van der Waals effect, thus increasing the probability of effective collision. However, the combined action of them has not been applied to the synthesis of NMAs.

In this work, we propose a new, easy, convenient, environmentally friendly and record-breaking method to rapidly synthesize NMAs. Combining the action of reducing agent $NaBH_4$ and ultrasonic wave to gelation process, under the cavitation of ultrasound, which generates huge energy with heating and stirring, gelation reaction can proceed rapidly, and even the process can be completed in only a few seconds, which is much faster than the reported before (Table S1 in Supporting information) [28]. It can successfully complete the gelation process in a wide concentration range (from 0.02 mmol/L to 62.5 mmol/L). It is suitable for various noble metal elements (Au, Ru, Rh, Ag, Pt, Pd), and can synthesize single metal aerogels (Au, Ag, Ru, Rh, Pd), bimetal and trimetal aerogels (Au-Ag, Au-Rh, Au-Ru, Au-Pt, Au-Pd, Au-Pt-Pd), while the ligament size of alloy aerogels is 10 nm or less. We also explored their outstanding electrocatalytic performance in HER and EOR.

Here, we introduced the synthesis process by taking the gold aerogel as an example. In the ultrasonic environment, the freshly prepared $NaBH_4$ solution was quickly poured into the $HAuCl_4$ solution (the molar ratio of the reducing agent to the metal is 10 c_{Au} = 2.0 mmol/L) and the system reacted quickly. From the reducing agent was added to the metal solution, we recorded the reaction of the system at 20 s, 35 s and 50 s respectively, and they were shown in Figs. 1a-d. As soon as the freshly prepared $NaBH_4$ aqueous solution was injected in the precursor solution, the system quickly began to react, showing a black color, with a lot of H_2 bubbles coming out, which was caused by the progress of the reduction reaction and situ-produced by $NaBH_4$. Next, when the reaction reached 20 s, there were a lot of black flocculent sediments and bubbles, and the black flocculent sediments tended to aggregate, but due to bubbles and the effect of ultrasound wave, these flocculent sedimentations did not aggregate in bulk, and the system was in a turbid state. With the reaction going on, at 35 s, the system became transparent slowly, the bubbles were reduced, and a small amount of black flocculent precipitates gathered. At 50 s, the solution was clear and transparent, and the black flocculent precipitates no longer formed. After leaving the ultrasonic environment, the black flocculent precipitates gathered into large floc-things. Compared with the reaction without ultrasonic field treatment, it took 2 h to end the reaction (Fig. S1 in Supporting information). Therefore, we have concluded that ultrasound can greatly increase the reaction rate, shorten the aerogels' synthesis time, and simplify the synthesis process. In order to verify that the aerogels have been successfully synthesized, we used transmission electron microscopy (TEM) to characterize the aerogels with different reaction times (Figs. 1e-g). From these images, we can observe that the gel network had initially formed within 20 s, and the scale

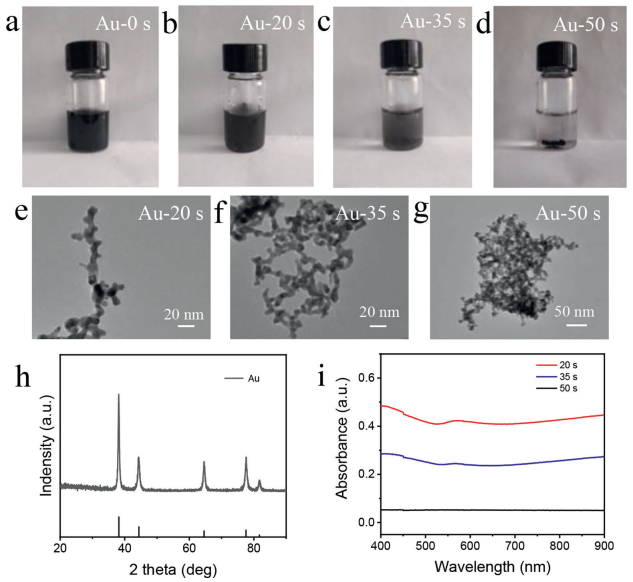

Fig. 1. Demonstration and characterization of Au aerogels by ultrasonic methods (c_M = 2 mmol/L). (a-d) Photographs of Au gelation process under different time (the reaction time is 50 s). (e-g) TEM images of Au aerogel corresponding time of 20 s, 35 s, and 50 s. (h) XRD spectrum of gold aerogel. (i) UV–vis absorption spectra displaying the gelation state.

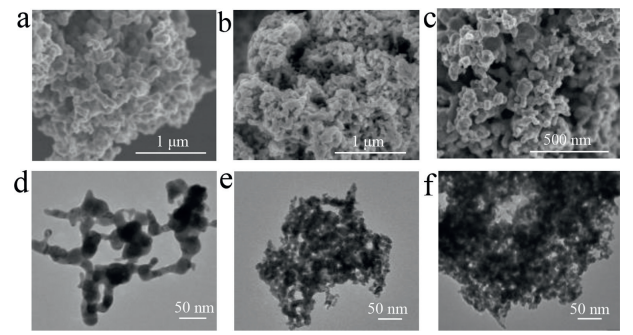

Fig. 2. Characterization of Au aerogels by ultrasonic methods under different power. (a-c) SEM images of Au aerogels under different power 340 W, 670 W, 840 W, respectively. (d-f) TEM images of Au aerogels under different power 340 W, 670 W, 840 W, respectively.

of the ligament increases rapidly over time. At the same time, we also performed X-ray diffraction (XRD) characterization of the synthesized gold aerogel (Fig. 1h). In addition, the ultraviolet-visible (UV–vis) absorption spectrum (Fig. 1i) in the range of 400–900 nm was also used to characterize the hydrogel formation process.

What is more, in order to ensure the unique variable and determine the optimal reaction conditions, we also conducted experiments on the influence of different ultrasonic powers on the gelation process. Under the ultrasonic power of 340 W, 670 W and 840 W, the reducing agent is rapidly injected into the metal precursor solution, respectively. It was found that the shortest time required for the gelation process was 50 s when the ultrasonic machine power was 840 W. At the same time, we also took scanning electron microcopy (SEM) (Figs. 2a-c) and TEM (Figs. 2d-f) images of the synthesized aerogels. As we can see, 3D self-supporting network structure was formed, and aerogels were porous and fluffy under dry state. It can be found that when the ultrasonic power was 840 W, the aerogel's network structure formed completely. The largest scale, longer ligaments, and smallest aerogels particles were conducive to expose more active sites and form finer electron transmission channels [35,38]. Further, we studied the gelation process in a wide concentration range of this method, from

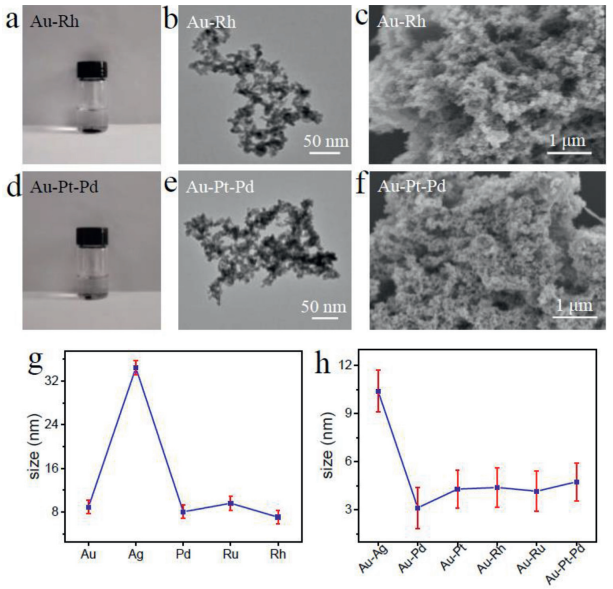

Fig. 3. (a, d) Photos of Au-Rh, Au-Pt-Pd. (b, e) TEM images of Au-Rh, Au-Pt-Pd. (c, f) SEM images of Au-Rh, Au-Pt-Pd. (g-h) Ligament size of single NMAs and alloy NMAs.

0.02 mmol/L to 62.5 mmol/L (Fig. S2 in Supporting information). In view of the most suitable ultrasonic power, we used 840 W ultrasonic power in the future experiment. Kept the amount of metal unchanged, and changed the molar ratio of reducing agent to metal was 5:1, 50:1 and 100:1 respectively, then recorded the reaction time when the $NaBH_4$ was different proportion under ultrasonic conditions (Fig. S3 in Supporting information). It was found that the lager molar ratio of the reducing agent, the shorter the reaction time would be spent. When the ratio of reducing agent to metal was 100:1, it only took 37 s to complete the gelation process. However, when the ratio was 5:1, it took a longer time, and even need to stand still to aggregate after the reaction. Fig. S4 (Supporting information) provided the nitrogen adsorption-desorption isotherms and pore size distribution with cumulative pore volume of Au aerogels. The Brunauer-Emmett-Teller (BET) surface area of the prepared gold aerogel was 4.65 m^2/g; as we can see, it mainly existed mesopores (2–50 nm) [35].

Inspired by the method that successfully prepared gold hydrogel with ultrasound and excess reducing agent $NaBH_4$, then this method was extended to the gelation process of other noble elements (Pt, Pd, Ag, Ru, Rh), which was used to shorten the preparation time of aerogels. Single-metal aerogels and bimetallic aerogels (Au-Rh) (Fig. 3a) and trimetallicaerogel (Au-Pd-Pt) (Fig. 3d) were being prepared and synthesized, and characterized by TEM images (Figs. 3b and e) and SEM images (Figs. 3c and f). And the high-resolution TEM (HR-TEM) images of Au-Rh aerogel and Au-Pt-Pd aerogel were displayed in Figs. S5 and S6 (Supporting information), respectively. Au-Rh aerogel mainly showed (111) crystal planes, while Au-Pt-Pd aerogel mainly exposed (111) crystal planes, too. We applied this excess reducing agent ultrasound method to the synthesis and preparation of single metal aerogels (Ru, Ag, Pd, Rh) and alloy aerogels (Au-Pd, Au-Pt, Au-Ag, Ag-Ru) in Figs. S7 and S8 (Supporting information), and performed characterization of TEM images (Figs. S9 and S10 in Supporting information). Moreover, the ligament size of single NMAs and alloy NMAs were shown in Figs. 3g-h. We analyzed the size of single-metal aerogels and alloy aerogels synthesized by ultrasound through TEM images. It was found that the ligament sizes of single metal aerogels (Au, Rh, Ru and Pd) were all similar in size around 10 nm, but Ag aerogels were about 34 nm. However, the ligament size of alloy aerogels (Au-Pt, Au-Pd, Au-Pt-Pd, Au-Rh, Au-Ru) are all about 6 nm, but the Au-Ag aerogel is about 11 nm.

From SEM images of these aerogel materials (Figs. S11 and S12 in Supporting information), we can see that a network-like pore structure with a large number of pore structures inside, which can expose more surface area and promote the penetration of the electrolyte solution. At the same time, this structure can accelerate the transfer of electrons, accelerate the diffusion of bubbles in the electrocatalytic hydrogen release reaction, and show excellent electrocatalytic performance. We also performed XRD (Figs. S13 and S14 in Supporting information) characterization of the prepared aerogels, by comparing the alloy aerogels with the single metal aerogels, it was found that the position of the alloy peak in the XRD was shifted, thus it was speculated that the aerogels have been successfully synthesized. In addition, it can be found that the peak intensity of Au and Ag are higher. The nice crystallinity can be attributed to the large ligament size. Among them, the ligament size of Ag could reach 34 nm. The signal-to-noise ratio of Rh, Ru, and Pd were comparatively lower. The reason is that the ligament size was relatively small, and the crystallinity were relatively poor. Moreover, Rh and Ru have spontaneous combustion characteristics when exposed to the air, and can form oxide species. Subsequently, we also performed X-ray photoelectron spectroscopy (XPS) (Fig. S15 in Supporting information) characterization for alloy aerogels. Analyzing the XPS spectra of Au-Rh aerogel and Au-Pt-Pd aerogel respectively (Figs. S16 and S17 in Supporting information), we found that due to the aerogels were long-term exposed to the air, there were not only a large number of 0 valence state, but also some oxidation states. The mapping and Energy dispersive X-ray spectroscopy (EDS) of the prepared aerogels Au-Rh, Au-Pt, Au-Pd, Au-Pt-Pd were respectively shown in Figs. S18-S21 (Supporting information) which demonstrated the elements uniformly distributed in the alloy aerogels.

In consideration of the rapidity of ultrasonically synthesizing aerogels, we explored the behavior of NMAs in the ultrasonic field, and highlighted the possible underlying mechanisms. At first, it was primary aggregates, and then slowly gathered into large scale. These large hydrogels sunk to the bottom of the container under the action of gravity. However, these building blocks are not stable. In an ultrasonic condition, these building blocks were dispersed into small pieces by ultrasound and floated in the solution, and so on, until the ultrasonic effect disappeared, and they reassembled at the bottom of the container. The NMAs can maintain high reactivity in the reaction environment, which is inseparable from the self-healing behavior of the aerogels, which also shows that the synthesized aerogels is self-supporting, not a precipitate [33]. In addition, the black color of the synthesized aerogels indicates that the multiple refraction and scattering of light has formed a small and hierarchical microstructure [30,40].

In ultrasonic machine, electric energy is converted into ultrasonic wave. it has strong penetrability in water, which acts inside the reactant, so that the reaction system and reactant work together to intensify the reaction. Furthermore, it can produce cavitation and produce huge energy, which generates huge energy with heating and stirring for the reaction system, thus speeding up the reaction. Furthermore, the high energy of ultrasonic also acts on the hydrogels itself, effectively destroying the self-healing behavior of the hydrogels, promoting more self-supporting network structures and effectively reducing the ligament size of the aerogels. The gelation process of the system with excess reducing agent $NaBH_4$ must consider the influence of ionic effects [30]. The excess salt satisfies the conditions for activating the target ion in the Hofmeister series [41]. $NaBH_4$ ionizes into Na^+ and BH_4^- in water. BH_4^- convert into BO_2^- in situ and generate a large number of H_2 bubbles surrounded by metal ions [35], this effect can be further strengthened under the action of ultrasound, and the whole

process is more intense. A large amount of Na^+ can adjust the fusion mode of metal ions, where the role of anions are even more important [42,43]. The BH_4^- around the metal nanoparticles was converted into BO_2^- in situ, which also reduces the concentration of metal ions due to the release of H_2. The size of this anion is small and the distance between its nuclei is small. Through van der Waals effect, the instability, the collisions between metal nanoparticles, and the probability of effective collisions can be incresed [35], while this van der Waals effect could be greatly enhanced by ultrasonic action. Therefore, the time of gelation process can be greatly shortened.

As the reducing agent decomposes in a large amount, the reaction gradually slows down until the solution becomes clear and transparent. After the reaction is over, the reaction system is taken out of the ultrasonic field, and the hydrogels building blocks are gathered together again. In Rh, Ru related single metal and bimetallic hydrogels, the solution is not clear after the gelation process is completed by ultrasound. This is not about no reaction, while the energy of ultrasound is higher than that of gravity. The formed hydrogels are dispersed into primary aggregates. After the ultrasound is over, these small hydrogels fragments will settle on the bottom of the reaction vessel after standing for about 10 min. We also found that its 3D network structure is very fine, and the particles are about 3 nm, much smaller than Au and Ag. This helps them expose more active sites and improve catalytic performance.

Since the NMAs can expose a large number of active sites, it forms a network structure with good electron transfer characteristics, which has an irreplaceable role for other materials in the field of electrocatalysis. In this paper, the synthesized aerogels are used for HER and EOR in alkaline medium.

The HER is a cathodic reaction in electrolyzed water, but due to its higher activation energy and overpotential [44–49], a catalyst is needed to reduce the activation energy and overpotential of its reaction, thereby increasing the reaction activity. Obviously, among the single metal and bimetallic aerogels that have been synthesized, Au-Rh aerogel has the best HER catalytic activity. In the three-electrode system, the saturated calomel electrode is used as the reference electrode, the carbon rod is the counter electrode, and the glassy carbon electrode of Au-Rh hydrogel catalyst ink is used as the working electrode. According to the same method, the working electrodes with Au-Rh NPs, Au-Ru aerogel, Rh aerogel, Au-Pt-Pd aerogel and commercial Pt/C as catalysts were prepared for comparison. The linear voltammetry scanning (LSV) can confirm that Au-Rh aerogel in 1.0 mol/L KOH electrolyte shows obvious HER activity as the current density of the negative electrode increases. The overpotential of Au-Rh aerogel is much lower than commercial Pt/C (Fig. 4a). The minimum overpotential of Au-Rh aerogel is 15.1 mV at 10 mA/cm^2 (Fig. S22 in Supporting information). The Tafel slopes of Au-Rh aerogel, Pt/C, AuRh NPs, AuRu aerogel, Rh aerogel, Au-Pt-Pd aerogel were shown in Fig. 4b. In addition, the Au-Rh catalyst was subjected to a 12-h chronoamperometry test (Fig. 4c), and it was found that its current density was in a stable state. In order to further verify the stability of the catalyst, after 10,000 cycles of the cyclic voltammograms (CVs), we tested the LSV of Au-Rh aerogel and found the catalytic activity hardly decreased (Fig. S23 in Supporting information), while the aerogels' structure in the TEM image and XRD (Fig. S24 in Supporting information) did not change after the reaction. These also show that the catalyst has brilliant properties and stability. In addition, the electric double layer capacitance (C_{dl}) of materials was shown in Fig. S25 (Supporting information). Au-Rh aerogel is 4.5 mF/cm^2, and the C_{dl} of Au-Rh NPs is 1.1 mF/cm^2. Among them, Au-Rh aerogel has the highest electric double layer capacitance, indicating a large number of macroporous active sites exposed. The HER performance of other aerogels materials were listed in the Table S2 (in Supporting information).

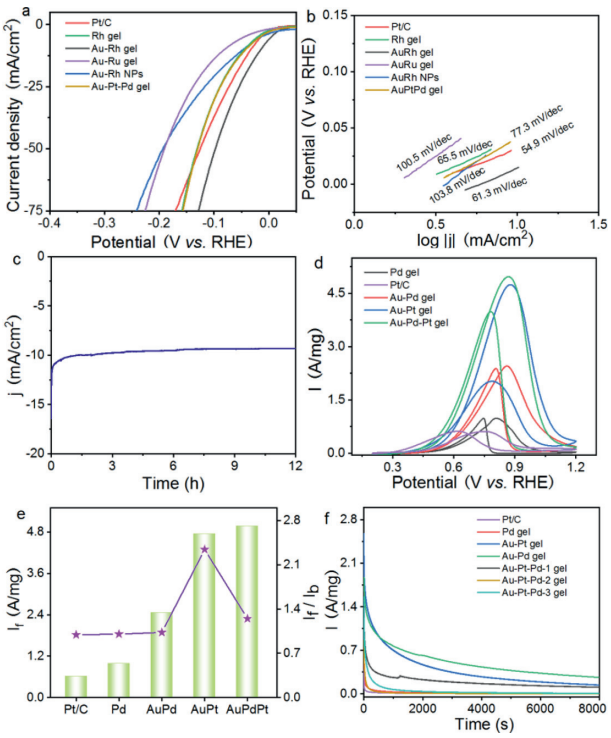

Fig. 4. (a-c) Electrocatalytic performance of HER in 1.0 mol/L KOH. (a) LSV curves with a scan rate of 5 mV/s. (b) Tafel plots. (c) Chronoamperometry tests in 1.0 mol/L KOH solution. (d-f) Electrocatalytic performance of EOR. (d) CV curves with a scan rate of 50 mV/s. (e) Summarized I_f and I_f/I_b. (f) Chronoamperometry tests of various aerogel catalysts in 1.0 mol/L KOH + 1.0 mol/L ethanol solution.

In addition to the HER reaction, the ethanol oxidation properties of NMAs were also studied. Before detecting EOR activity, we calculated the electrochemically active surface areas (ECSA) based on charges involved in the adsorption of hydrogen in the CVs recorded in 1.0 mol/L KOH, which were 23.4, 27.6, 21.8, 37.2 m^2/g for Pd aerogel, Au-Pd aerogel, Au-Pt aerogel, Au-Pt-Pd aerogel shown in Fig. S26 (Supporting information). The catalyst materials involved are Pd aerogel, Au-Pt aerogel, Au-Pd aerogel, Au-Pt-Pd aerogel and commercial Pt/C. In the three-electrode system, the electrolyte containing ethanol is saturated with N_2 in advance, and then the electrochemical test is performed. When scanning by cyclic voltammetry, there are two peaks in forward and backward scanning (Fig. 4d), which respectively represent the oxidation of ethanol and the further oxidation of intermediates. The forward scanning current (I_f) of Au-Pt-Pd is 4.97 A/mg, and the ratio of forward current to reverse current (I_f/I_b) is 1.27. Compared with Au-Pt-Pd aerogel, commercial Pt/C (0.67 A/mg 0.92), Au-Pd (2.45 A/mg 1.02), Pd (0.98 A/mg 1.0) are poorer (Fig. 4e). What is more, the stability of these catalysts was also verified, and they can maintain good stability at a constant potential of 8000 s (Fig. 4f). TEM images and XRD pattern (Fig. S27 in Supporting information) were taken after chronoamperometry tests. It was found that the aerogels' structure was not destroyed after the reaction, which also showed that the catalyst was outstanding stability. The EOR performance of other aerogels materials were listed in the Table S3 (Supporting information).

To sum up, we propose a new easy, convenient, environmentally friendly and record-breaking method to rapidly synthesis NMAs. Combining the action of reducing agent $NaBH_4$ and ultrasonic wave to gelation process, under the cavitation of ultrasound, which generates huge energy with heating and stirring. The gelation reaction can proceed rapidly, and even can be completed in only a few seconds, which is much faster than reported before

(Table S1). It can successfully complete the gelation process in a wide concentration range (0.02–62.5 mmol/L). This method is suitable for the synthesis of single metal aerogels (Au, Ag, Ru, Rh, Pd), bimetal and trimetal aerogels (Au-Ag, Au-Rh, Au-Ru, Au-Pt, Au-Pd, Au-Pt-Pd), while the ligament size of alloy aerogels is 10 nm or less. We also verified their outstanding electrocatalytic performance in HER and EOR. The above experiments show that the rapid and effective synthesis method of NMAs is conducive to its further applications in electrocatalysis field.

Declaration of competing interest

The authors declare that they have no known competing financial interests or personal relationships that could have appeared to influence the work reported in this paper.

Acknowledgments

This research was sponsored by the National Natural Science Foundation of China (Nos. 51772162, 22001143 and 52072197), Youth Innovation and Technology Foundation of Shandong Higher Education Institutions, China (No. 2019KJC004), Outstanding Youth Foundation of Shandong Province, China (No. ZR2019JQ14), Taishan Scholar Young Talent Program (Nos. tsqn201909114, tsqn201909123), Natural Science Foundation of Shandong Province (No. ZR2020YQ34), Major Scientific and Technological Innovation Project (No. 2019JZZY020405), and Major Basic Research Program of Natural Science Foundation of Shandong Province (No. ZR2020ZD09).

Supplementary materials

Supplementary material associated with this article can be found, in the online version, at doi:10.1016/j.cclet.2021.09.104.

References

[1] J.N. Tiwari, A.M. Harzandi, M. Ha, et al., Adv. Energy Mater. 9 (2019) 1970101.
[2] W. Fu, Y. Wang, J. Hu, et al., Angew. Chem. Int. Ed. 58 (2019) 17709–17717.
[3] P.S. Pálvölgyi, D. Sebők, I. Szenti, et al., Nano Res 14 (2021) 1450–1456.
[4] T. Li, D. Zhi, Y. Chen, et al., Nano Res. 13 (2020) 477–484.
[5] J. Biener, M. Stadermann, M. Suss, et al., Energy Environ. Sci. 4 (2011) 656–667.
[6] C. Ziegler, A. Wolf, W. Liu, et al., Angew. Chem. Int. Ed. 56 (2017) 13200–13221.
[7] V. Sayevich, B. Cai, A. Benad, et al., Angew. Chem. Int. Ed. 55 (2016) 6334–6338.
[8] X. Hu, W. Xu, L. Zhou, et al., Adv. Mater. 29 (2016) 1604031.
[9] A. Hitihami-Mudiyanselage, K. Senevirathne, S.L. Brock, ACS Nano 7 (2013) 1163–1170.
[10] H. Hu, Z. Zhao, W. Wan, et al., Adv. Mater. 25 (2013) 2219–2223.
[11] K.G.S. Ranmohotti, X. Gao, I.U. Arachchige, Chem. Mater. 25 (2013) 3528–3534.
[12] H.W. Liang, Q.F. Guan, L.F. Chen, et al., Angew. Chem. Int. Ed. 51 (2012) 5101–5105.
[13] J. Pan, S. Song, J. Li, et al., Nano Res. 10 (2017) 3486–3495.
[14] R. Du, X. Jin, R. Hübner, et al., Adv. Energy Mater. 10 (2019) 1901945.
[15] V. Zielasek, B. Jürgens, C. Schulz, et al., Angew. Chem. Int. Ed. 45 (2006) 8241–8244.
[16] N. Leventis, N. Chandrasekaran, C. Sotiriou-Leventis, et al., J. Mater. Chem. 19 (2009) 63–65.
[17] H. Bi, T. Lin, F. Xu, et al., Nano Lett. 16 (2015) 349–354.
[18] V. Lesnyak, A. Wolf, A. Dubavik, et al., J. Am. Chem. Soc. 133 (2011) 13413–13420.
[19] B.C. Tappan, S.A. Steiner III, E.P. Luther, Angew. Chem. Int. Ed. 49 (2010) 4544–4565.
[20] J.P. Vareda, A. Lamy-Mendes, L. Durães, Micropor. Mesopor. Mater. 258 (2018) 211–216.
[21] S. Shi, B. Qian, X. Wu, et al., Angew. Chem. Int. Ed. 58 (2019) 18171–18176.
[22] T. Raj kumar, G. Gnana kumar, A. Manthiram, Adv. Energy Mater. 9 (2019) 1803238.
[23] B. Cai, R. Hübner, K. Sasaki, et al., Angew. Chem. Int. Ed. 57 (2018) 2963–2966.
[24] N.C. Bigall, A.K. Herrmann, M. Vogel, et al., Angew. Chem. Int. Ed. 48 (2009) 9731–9734.
[25] F. Gao, L. Viry, M. Maugey, et al., Nat. Commun. 1 (2010) 2.
[26] S. Henning, H. Ishikawa, L. Kühn, et al., Angew. Chem. Int. Ed. 28 (2017) 10707–10710.
[27] H. Wang, Y. Wu, X. Luo, et al., Nanoscale 11 (2019) 10575–10580.
[28] F.J. Burpo, E.A. Nagelli, L.A. Morris, et al., J. Mater. Res. 32 (2017) 4153–4165.
[29] S.D. Minteer, B.Y. Liaw, M.J. Cooney, Curr. Opinion Biotech. 18 (2007) 228–234.
[30] R. Du, Y. Hu, R. Hübner, et al., Sci. Adv. 5 (2019) eaaw4590.
[31] K. Liu, Z. Nie, N. Zhao, et al., Science 329 (2010) 197–200.
[32] I.U. Arachchige, S.L. Brock, Acc. Chem. Res. 40 (2007) 801–809.
[33] R. Du, X. Fan, X. Jin, et al., Matter 1 (2019) 39–56.
[34] W. Liu, P. Rodriguez, L. Borchardt, et al., Angew. Chem. Int. Ed. 52 (2013) 9849–9852.
[35] R. Du, J. Wang, Y. Wang, et al., Nat Commun. 11 (2020) 1590.
[36] X. Gao, R.J. Esteves, T.T.H. Luong, et al., J. Am. Chem. Soc. 136 (2014) 7993–8002.
[37] D. Wen, W. Liu, D. Haubold, et al., ACS Nano 10 (2016) 2559–2567.
[38] R. Du, J.-.O. Joswig, R. Hübner, et al., Angew. Chem. Int. Ed. 59 (2020) 8293–8300.
[39] Y. Lin, F. Liu, G. Casano, et al., Adv. Mater. 28 (2016) 7993–8000.
[40] T. Sondergaard, S.M. Novikov, T. Holmgaard, et al., Nat. Commun. 3 (2012) 969.
[41] M. Bostrom, D.R. Williams, B.W. Ninham, Phys. Rev. Lett. 87 (2001) 168103.
[42] M.G. Cacace, E.M. Landau, J.J. Ramsden, Q. Rev. Bio. 30 (1997) 241–277.
[43] A. Nag, M.V. Kovalenko, J.S. Lee, et al., J. Am. Chem. Soc. 133 (2011) 10612–10620.
[44] P. Yu, F. Wang, T.A. Shifa, et al., Nano Energy 58 (2019) 244–276.
[45] J. Yu, Q. He, G. Yang, et al., ACS Catal. 9 (2019) 9973–10011.
[46] S. Anantharaj, V. Aravindan, Adv. Energy Mater. 10 (2020) 1902666.
[47] D. Zhang, Y. Shi, H. Zhao, et al., J. Mater. Chem. A 9 (2021) 889–893.
[48] D. Zhang, H. Zhao, B. Huang, et al., ACS Cent. Sci. 5 (2019) 1991–1997.
[49] Q. Chen, Y. Nie, M. Ming, et al., Chin. J. Catal. 41 (2020) 1791–1811.